Published in final edited form as:

FASEB J. 2008 June ; 22(6): 2023–2036. doi:10.1096/fj.07-099697.

Hydrogen peroxide inhibits Ca^{2+}-dependent chloride secretion across colonic epithelial cells *via* distinct kinase signaling pathways and ion transport proteins

Alfred E. Chappell[*], **Michael Bunz**[*,1], **Eric Smoll**[*], **Hui Dong**[*], **Christian Lytle**[†], **Kim E. Barrett**[*], and **Declan F. McCole**[*,2]

[*]Division of Gastroenterology, Department of Medicine, University of California, San Diego, School of Medicine, La Jolla, California, USA

[†]Division of Biomedical Sciences, University of California, Riverside, California, USA

Abstract

Reactive oxygen species (ROS) are key mediators in a number of inflammatory conditions, including inflammatory bowel disease (IBD). ROS, including hydrogen peroxide (H_2O_2), modulate intestinal epithelial ion transport and are believed to contribute to IBD-associated diarrhea. Intestinal crypt fluid secretion, driven by electrogenic Cl^- secretion, hydrates and sterilizes the crypt, thus reducing bacterial adherence. Here, we show that pathophysiological concentrations of H_2O_2 inhibit Ca^{2+}-dependent Cl^- secretion across T_{84} colonic epithelial cells by elevating cytosolic Ca^{2+}, which contributes to activation of two distinct signaling pathways. One involves recruitment of the Ca^{2+}-responsive kinases, Src and Pyk-2, as well as extracellular signal-regulated kinase (ERK). A separate pathway recruits p38 MAP kinase and phosphoinositide 3-kinase (PI3-K) signaling. The ion transport response to Ca^{2+}-dependent stimuli is mediated in part by K^+ efflux through basolateral K^+ channels and Cl^- uptake by the Na^+-K^+-$2Cl^-$ cotransporter, NKCC1. We demonstrate that H_2O_2 inhibits Ca^{2+}-dependent basolateral K^+ efflux and also inhibits NKCC1 activity independently of inhibitory effects on apical Cl^- conductance. Thus, we have demonstrated that H_2O_2 inhibits Ca^{2+}-dependent Cl^- secretion through multiple negative regulatory signaling pathways and inhibition of specific ion transporters. These findings increase our understanding of mechanisms by which inflammation disturbs intestinal epithelial function and contributes to intestinal pathophysiology.—Chappell, A. E., Bunz, M., Smoll, E., Dong, H., Lytle, C., Barrett, K. E., McCole, D. F. Hydrogen peroxide inhibits Ca^{2+}-dependent chloride secretion across colonic epithelial cells *via* distinct kinase signaling pathways and ion transport proteins. *FASEB J.* 22, 000–000 (2008)

Keywords

reactive oxygen species; PI3-kinase; MAP kinases; NKCC1

[2]Correspondence: Division of Gastroenterology, University of California, San Diego, 9500 Gilman Dr., La Jolla, CA 92093-0063, USA. dmccole@ucsd.edu.

[1]Current address: Medical Faculty, University of Regensburg, Franz-Josef-Strauss-Allee 11, 93042 Regensburg, Germany.

THE GENERATION OF reactive oxygen species (ROS) is believed to play a prominent role in the mediation of injury and loss of function associated with a number of intestinal inflammatory conditions, including inflammatory bowel disease (IBD). Although the pathophysiology of IBD has not been fully elucidated, a growing body of clinical and experimental data suggests that the chronic inflammation associated with IBD may result from an inappropriate immune response to normal bacterial antigens. The dysregulated immune response results in the sustained overproduction of reactive metabolites of oxygen and nitrogen (1, 2). Data obtained from several studies indicate that chronically inflamed colonic tissue is subject to significant oxidative stress (3–6). The uncontrolled overproduction of ROS, as occurs during active episodes of IBD, can overwhelm protective antioxidant mechanisms, resulting in oxidative damage to cells and tissues. A number of studies have shown reduced levels of antioxidant enzymes, such as superoxide dismutase (SOD), in patients with Crohn's disease (7) and increased oxidized glutathione in ulcerative colitis (UC) patients (8). In addition, there are comparatively low levels of endogenous antioxidants in the colonic mucosa, with the majority of the enzymatic antioxidant production in the colon occurring in the epithelium and little produced in the lamina propria (2). Moreover, a number of antioxidants have been shown to protect against the onset of diarrhea in mouse models of colitis (9–11).

Of the ROS believed to have a role in IBD, hydrogen peroxide (H_2O_2) is one that has been the subject of much investigation. H_2O_2 can be formed by the dismutation of superoxide or the two electron reduction of oxygen. The large number of activated phagocytes commonly found in ulcerative colitis may secrete millimolar concentrations of H_2O_2 in close proximity to colonocytes (12). H_2O_2 *per se* can react with lipids and sulfhydryls to inactivate key enzymes (13, 14). At physiological concentrations, H_2O_2 not only can cause direct damage to cultured epithelial cells and cells isolated from IBD patients, but also, along with superoxide, can interact with low-molecular-weight, redoxactive forms of iron to yield the highly reactive hydroxyl radical that also damages epithelial cells *in vitro* (2, 7, 15). Following activation of neutrophils and monocytes, H_2O_2 will also result in enhanced formation of the potent oxidant, hypochlorous acid (HOCl) from myeloperoxidase (MPO)-catalyzed oxidation of Cl^- by H_2O_2 (13). H_2O_2 is therefore an important precursor of a number of very damaging ROS.

Despite evidence that many inflammatory mediators such as eicosanoids, histamine, and complement factors can activate ion transport in isolated intestine, intestinal tissues isolated from IBD patients, as well as mouse models of disease, exhibit a reduced ability to transport ions (16–20). This is believed to be a major factor in the diarrhea associated with IBD. A number of studies have investigated the effects of ROS on intestinal secretion (21). Studies in rat colonic tissue have shown that H_2O_2 can indirectly increase mucosal Cl^- secretion by causing the release of prostaglandins. These subsequently act on submucosal cholinergic neurons to stimulate the release of neurotransmitters (*i.e.*, acetylcholine) that evoke secretion, rather than acting directly on the epithelium (22, 23). A direct effect of H_2O_2 on Cl^- secretion has also been investigated using T_{84} colonic epithelial cells (24). A high concentration of H_2O_2 (5.5 mmol/L) was required to evoke a small increase in short-circuit current (I_{sc}), reflective of chloride secretion in this model. This study, and one by DuVall *et al.* (25), showed that H_2O_2 pretreatment of T_{84} cells for 30 min could also attenuate cAMP-

dependent Cl^- secretory responses. Importantly, the concentration of H_2O_2 used (500 μM), inhibited Cl^- secretion through specific effects on the Cl^- secretory pathway and did not affect paracellular permeability, nor prove toxic. The DuVall *et al.* study concluded that the principal effect of H_2O_2 on colonic cAMP-dependent Cl^- secretion was inhibitory. This has been supported by the work of Walker *et al.* (26). Other oxidants such as HOCl and NH_2Cl have been shown to increase colonic epithelial cell line and rat mucosal Cl^- secretion, as well as mucosal permeability (27–29). Studies have also shown that in some cell systems H_2O_2 can activate mitogen-activated protein (MAP) kinases, thus modulating cell growth. Our laboratory has established that a number of signaling kinases including members of the MAP kinase family, as well as nonreceptor tyrosine kinases, including Src, can negatively regulate intestinal chloride secretion (30, 31). However, the signaling mechanisms by which ROS influence colonic ion transport have not been well characterized. Therefore, in the present study we investigated the effects of ROS, specifically H_2O_2, on Ca^{2+}-dependent Cl^- secretion across colonic epithelial cells and the signaling pathways activated by H_2O_2 that modify epithelial ion transport responses.

MATERIALS AND METHODS

Materials

Carbachol (Sigma), tyrphostin AG1478, PP2, wortmannin, LY294002, PD98059, U0126, SB203580, H_2O_2 (Calbiochem, San Diego, CA, USA), mouse anti-human epidermal growth factor receptor (EGFR) (clone LA1) and mouse anti-phosphotyrosine antibodies (Upstate Biotechnology, Lake Placid, NY, USA), rabbit anti-phospho-Pyk-2 antibodies (Biosource International, Camarillo, CA, USA), anti-phospho-ERK antibodies (New England Biolabs, MA, USA) and Tris-glycine electrophoresis gels (Bio-Rad, Hercules, CA, USA) were obtained from the sources noted. Rabbit polyclonal anti-human EGFR (1005) and rabbit polyclonal anti-human ERK 1 (K-23) were used to measure total EGFR and ERK, respectively (Santa Cruz Biotechnology, Santa Cruz, CA, USA). All other reagents were of analytical grade and obtained commercially.

Cell culture

Methods for maintenance of T_{84} cells in culture were described previously (32). Briefly, T_{84} cells were grown in Dulbecco's modified Eagle's/F-12 medium (DMEM/F12) (Mediatech Inc., Herndon, VA, USA) supplemented with 5% newborn calf serum. For Ussing chamber/voltage-clamp experiments, 5×10^5 cells were seeded onto 12-mm Millicell transwell polycarbonate filters. For Western blot analysis experiments, 10^6 cells were seeded onto 30-mm filters. Cells were cultured for 10–15 days prior to use. When grown on polycarbonate filters, T_{84} cells are known to acquire the polarized phenotype of native colonic epithelia. In accordance with muscarinic M3 receptors, distribution on intestinal epithelia, carbachol (CCh) was added basolaterally in all experiments.

HT-29.cl19A cells (33) were grown to confluence (~5 days) in DMEM supplemented with 10% FBS, l-glutamine, and streptomycin in 75 cm^2 flasks. After the cells had reached confluence, they were seeded onto 12-mm round coverslips (Warner Instruments Inc., Hamden, CT, USA) and incubated for at least 24 h before use.

Physiological solutions

The composition of the Ringer's solution used for Ussing chamber, Western blot studies, and $^{86}Rb^+$ uptake studies was (in mM): 140 Na^+, 120 Cl^-, 5.2 K^+, 25 HCO_3^-, 0.4 $H_2PO_4^-$, 2.4 HPO_4^{2-}, 1.2 Ca^{2+}, 1.2 Mg^{2+}, and 10 D-glucose. The physiological salt solution used in digital Ca^{2+} measurement contained the following (in mM): 140 Na^+, 5.0 K^+, 2.0 Ca^{2+}, 147 Cl^-, 10 HEPES, and 10 glucose. The solution osmolality was ~284 mosmol/kg. HEPES-buffered Hank's balanced salt solution (HBSS) was used in $^{86}Rb^+$ efflux experiments. The HBSS composition was (in mM): 137 NaCl, 5.4 KCl, 0.4 KH_2PO_4, 0.3 Na_2HPO_4, 1.0 $MgCl_2$, 1.0 $CaCl_2$, 15 HEPES, pH 7.2, and 10 D-glucose). The chloride-free buffer used in $^{86}Rb^+$ uptake studies contained (in mM): 2.4 K_2HPO_4, 0.4 KH_2PO_4, 25 $NaHCO_3$, 1.2 $MgSO_4$, 1.2 mM $CaSO_4$, 115 sodium isethionate, and 10 D-glucose.

Electrophysiological studies

T_{84} cells grown to confluence on permeable 12-mm filters were mounted in Ussing chambers (window area = 0.6 cm^2) and bathed in oxygenated (95% O_2–5% CO_2) Ringer's solution at 37°C. Monolayers were voltage-clamped to zero potential difference by the application of short-circuit current (I_{sc}). Under these conditions, changes in I_{sc} (ΔI_{sc}) in response to agonists are wholly reflective of electrogenic chloride secretion (34). Transepithelial resistance (TER) was measured using a "chopstick" voltohmeter (World Precision Instruments, Sarasota, FL, USA) (35). The MAPK inhibitor, SB203580, and the MEK inhibitor, PD98059, were solubilized in dimethyl sulfoxide (DMSO). In control studies, the final concentration of DMSO (0.1%) had no effect on I_{sc} responses to CCh in the presence or absence of H_2O_2 (data not shown). This is in keeping with our previous unpublished findings and with studies by other groups on MAPK phosphorylation using intestinal epithelial cell lines (36). Thus, later studies were conducted without DMSO addition to control solutions.

Immunoprecipitation and Western blot analysis

T_{84} cell monolayers were washed (3×) with Ringer's solution, allowed to equilibrate for 30 min at 37°C and were then stimulated with agonists (±antagonists) as appropriate. The reaction was stopped by washing in ice-cold PBS, and the cells were lysed in ice-cold lysis buffer (1% Triton X-100, 1 μg/ml leupeptin, 1 μg/ml pepstatin, 1 μg/ml antipain, 100 μg/ml phenylmethylsulfonyl fluoride, 1 mM Na^+-vanadate, 1 mM sodium fluoride, and 1 mM EDTA in phosphate buffered saline) for 45 min. Cell lysate supernatants were assayed for protein content (Bio-Rad protein assay kit) and adjusted so that each sample contained an equal amount of protein. For immunoprecipitation studies, lysates were incubated with immunoprecipitating antibody, as per the manufacturer's instructions, for 1 h at 4°C followed by another 1 h incubation at 4°C with protein A-Sepharose. Lysates were then centrifuged for 3 min at 15,000 relative centrifugal force, and the supernatant was discarded. The pellets were washed in ice-cold phosphate-buffered saline (3×) and resuspended in 2× gel-loading buffer (50 mM Tris, pH 6.8, 2% SDS, 200 mM dithiothreitol, 40% glycerol, 0.2 bromphenol blue) and boiled prior to separation by SDS-PAGE. Resolved proteins were transferred onto polyvinylidene membranes (NEN Life Science Products Inc., Boston, MA, USA). After transfer, the membrane was preblocked with a 1% solution of blocking buffer

(Upstate Biotechnology Inc.) for 30 min followed by 1 h incubation with the appropriate concentration of primary antibody in 1% blocking buffer. After washing (5×10 min) in Tris-buffered saline with 1% Tween (TBST), membranes were incubated for 30 min with a horseradish peroxidase-conjugated secondary antibody (anti-mouse or anti-rabbit IgG; BD Biosciences, San Jose, CA, USA) in 1% blocking buffer. After washing in TBST (5×10 min), immunoreactive proteins were detected using an enhanced chemiluminescence detection kit (GE Healthcare UK Ltd., Little Chalfont, UK). Densitometric analysis of Western blots was carried out using National Institutes of Health image software.

Digital Ca^{2+}imaging

$[Ca^{2+}]_{cyt}$ levels in HT-29.cl19A cells were measured by Fura-2 fluorescence ratio digital imaging, as described previously (37, 38). Briefly, HT-29.cl19A cells, grown on coverslips, were loaded with 5 μM Fura-2 acetoxymethyl ester (AM) (dissolved in 0.01% Pluronic F-127 plus 0.1% DMSO in physiological salt solution described previously) at room temperature for 50 min, then washed in normal physiological salt solution for at least 20 min. Thereafter, the coverslips were mounted in a perfusion chamber on a Nikon microscope stage. Cells were initially perfused with a normal physiological salt solution for 5 min, then perfused with the same solution containing H_2O_2 (500 μM). After that, H_2O_2 was washed out briefly, followed by treatment with CCh (100 μM) in normal physiological solution. The ratio of Fura-2 fluorescence with excitation at 340 or 380 nm ($F_{340/380}$) was followed over time and captured using an intensified charge-coupled device camera (ICCD200) and a MetaFluor Imaging System (Universal Imaging, Corporation, Downingtown, PA, USA).

Basolateral $^{86}Rb^+$ efflux studies

Basolateral K^+ efflux was measured using $^{86}Rb^+$ as a tracer in a method adapted from that described by Venglarik *et al.*(39). Briefly, confluent monolayers of T_{84} cells grown on 12-mm transwell inserts were rinsed 3× with HBSS, and incubated at 37°C for 20 min. Cells were loaded with $^{86}Rb^+$ by incubating for 40 min bilaterally with 1 μCi/ml $^{86}Rb^+$ in HBSS. After loading with $^{86}Rb^+$, cells were washed 3× with fresh HBSS and treated bilaterally with HBSS or H_2O_2 (500 μM) prepared in HBSS, for 30 min. Starting at 22 min into the 30-min incubation with HBSS±H_2O_2 (*i.e.*, t=8 min), inserts were transferred to new identical basolateral solutions every 2 min. At t=0, inserts were transferred to basolateral solutions of HBSS or 100 μM CCh prepared in HBSS with or without H_2O_2 and continued to be transferred to new identical basolateral solutions every 2 min for 14 min. At t=14 min, inserts were transferred directly into 5 ml scintillation fluid. Basolateral solutions at each time point were also transferred into 5 ml scintillation fluid, and $^{86}Rb^+$ content of the inserts and each 2-min basolateral fraction was measured using standard scintillation methods. The following equation was used to calculate the apparent rate constant: $r = [\ln(R1) - \ln(R2)]/(t1 - t2)$, where R1 and R2 are the percentage counts remaining in the cell monolayer at times t1 and t2, respectively. Data were expressed as rate of efflux per minute.

Basolateral $^{86}Rb^+$ uptake studies

Basolateral K^+ uptake was measured with $^{86}Rb^+$ as a tracer, using an adaptation of a previously described method (40). Confluent monolayers of T_{84} cells grown on 12-mm transwell inserts were rinsed 3× with warm Ringer's solution and incubated for 1 h at 37°C.

After 1 h preincubation, Ringer's solution was added bilaterally, or cells were treated bilaterally with H_2O_2 (500 μM) prepared in Ringer's solution, for 30 min on a warming plate at 37°C. Inserts were transferred to wells containing basolateral treatment solutions of Ringer's or 100 μM (CCh) prepared in Ringer's solution for 1 min, and then transferred to wells with basolateral uptake solutions containing 1 μCi/ml $^{86}Rb^+$ in either Ringer's solution or CCh prepared in Ringer's solution, and maintained at 37°C for 3 min. $^{86}Rb^+$ uptake was terminated by immersing inserts several times in ice-cold 100 mM $MgCl_2$ prepared in 10 mM Tris-HCl, pH 7.5. Filters were immediately excised from the inserts, placed directly into 5 ml scintillation fluid, and $^{86}Rb^+$ content was measured by standard scintillation methods. Experiments assessing bumetanide-sensitive uptake included 10 μM bumetanide (Sigma, St. Louis, MO, USA) in the basolateral treatment and uptake solutions. In experiments with chloride-depleted cells, except for the $^{86}Rb^+$ uptake solutions, Ringer's solution was replaced in the above procedures with a chloride-free buffer (composition shown above). The $^{86}Rb^+$ uptake solutions were prepared in normal Cl^--containing Ringer's solution. 86Rb $^+$ uptake was used to calculate K^+ uptake, for which it acts as a tracer (41). K^+ influx was calculated as (cpm/g protein/min)/SA, where SA is the specific activity of the uptake buffer (cpm/μmol K^+). Data were expressed as μmol of K^+ influx/g protein/min.

Statistical analysis

All data are expressed as means ± SE for a series of *n* experiments. Student's *t* test or analysis of variance (ANOVA) with the Student-Newman-Keuls post-test were used to compare mean values as appropriate. Values of $P<0.05$ were considered to represent significant differences.

RESULTS

H_2O_2 inhibits CCh-stimulated Cl^- secretion across T_{84} cells

H_2O_2 has previously been shown to inhibit cAMP-dependent Cl^- secretion across colonic epithelial cells; however, the effects of H_2O_2 treatment on Ca^{2+}-dependent Cl^- secretion have not been investigated. We initially set out to determine whether H_2O_2 could also inhibit the ability of epithelial cells to transport Cl^- in response to a calcium-dependent stimulus. Confluent monolayers of T_{84} colonic epithelial cells, grown on permeable supports, were mounted in Ussing chambers and pretreated bilaterally for 30 min with a range of concentrations of H_2O_2 (1–500 μM). The muscarinic agonist, CCh, was used as a prototypic receptor-mediated calcium-dependent secretagogue. The Cl^- secretory response to CCh, expressed as change in short circuit current (ΔI_{sc}), was not affected by H_2O_2 up to 100 μM. However, pretreatment with 500 μM H_2O_2 significantly inhibited the peak Cl^- secretory response to CCh (Fig. 1A; $P<0.01$ *vs.* CCh alone, open box; $n = 6$). Since 500 μM was the minimum effective concentration of H_2O_2 capable of inhibiting CCh-stimulated secretion, this concentration was used in all subsequent experiments. Figure 1B shows a time course of H_2O_2 (500 μM) pretreatment on CCh-stimulated I_{sc}. H_2O_2 pretreatment for 15 min caused a dramatic reduction in the peak ion transport response to CCh ($P<0.05$ *vs.* CCh alone; $n = 4$), while maximal inhibition was achieved with 30 min preincubation ($P<0.05$ *vs.* CCh alone; $n = 4$). H_2O_2 pretreatment for 30 min was used in all subsequent experiments. Figure 1C shows a time course of the I_{sc} response to CCh in the presence and absence of H_2O_2

pretreatment. H_2O_2 reduced the magnitude, but not the duration, of the Cl^- secretory response to CCh. To verify that the presence of H_2O_2 in the bathing media did not reduce the efficacy of CCh itself to stimulate ion transport through chemical modification of the ligand, we performed washout experiments in which the basolateral and apical bathing media containing H_2O_2, were replaced with fresh Ringer's solution. After a brief period of stabilization (5 min), CCh was added basolaterally. Figure 1D demonstrates that there was no difference in the inhibitory effect of H_2O_2 on CCh-stimulated I_{sc} in inserts that had been washed with fresh Ringer's solution *vs.* inserts that still contained H_2O_2 in the bathing media. These data indicate that H_2O_2 inhibits CCh-stimulated I_{sc} through effects on epithelial cells and not by altering the pharmacologic efficacy of CCh itself. Because H_2O_2 has been shown in certain studies to induce damage to epithelial monolayers, albeit at either higher concentrations, or following longer periods of incubation than used in the current studies (15, 42), we investigated whether incubation of T_{84} monolayers with H_2O_2 (500 μM) had any effect on the electrical resistance of the monolayer, as a measure of epithelial barrier integrity. Incubation of T_{84} monolayers with H_2O_2 for 30 min had no effect on TER of the monolayers when compared with Ringer's solution alone (Fig. 1E). These data show that H_2O_2 inhibits Ca^{2+}-dependent Cl^- secretion across intestinal epithelial cells in the absence of any obvious defects in monolayer integrity.

The role of MAPK signaling pathways in H_2O_2 inhibition of Ca^{2+}-dependent Cl^+secretion

We have previously shown important roles for MAPK signaling pathways in the negative regulation of GPCR-stimulated, Ca^{2+}-dependent Cl^- secretion across colonic epithelial cells (18, 30, 43). H_2O_2 has also been shown to activate MAPK signaling in other cell systems (44, 45). Consequently, we investigated whether the inhibitory effects of H_2O_2 on CCh-stimulated Cl^- secretion incorporated established MAPK signaling pathways involved in the regulation of Ca^{2+}-dependent Cl^- secretion. Preincubation for 30 min with PD98059 (20 μM), an inhibitor of the ERK-activating kinase, MEK, significantly reduced the inhibitory effect of H_2O_2 on CCh-stimulated ion transport across T_{84} cells (Fig. 2A, peak ΔI_{sc}, $P<0.05$; and Fig. 2B, time course; $P<0.01$; $n = 7$). These data were supported by an alternative MEK inhibitor, U0126 (Fig. 2C; $P<0.05$ *vs.* H_2O_2 CCh). To verify that H_2O_2 increased ERK activation and to determine the kinetics of activation, T_{84} monolayers were bilaterally treated with H_2O_2 (500 μM), and cell lysates were separated by SDS-PAGE, and resulting blots were probed for phosphorylated ERK (Thr204/Tyr 202). H_2O_2 transiently increased ERK phosphorylation, which was maximal at 5 min and returned to baseline by 30 min (Fig. 2D; $P<0.001$; $n = 4$).

As p38 MAPK is also involved in the negative regulation of Ca^{2+}-dependent Cl^- secretion (46), we next investigated whether p38 was involved in the inhibitory effect of H_2O_2 on CCh-stimulated Cl^- secretion. Preincubation of T_{84} monolayers with the p38 inhibitor, SB203580 (10 μM), for 30 min significantly reduced the inhibitory effect of H_2O_2 on Cl^- secretion, thus indicating a prominent role for p38 in mediating the inhibitory effect of H_2O_2 (Fig. 2F; $P<0.05$; $n = 5$). H_2O_2 actually caused a biphasic increase in p38 phosphorylation with significant increases at 0.5 and 5 min post H_2O_2 treatment (Fig. 2E; $P<0.05$; $n = 6$). These data indicate that the MAPKs, ERK and p38, are involved in mediating the inhibitory effect of H_2O_2 on Ca^{2+}-dependent Cl^- secretion.

Involvement of Src and Pyk-2 signaling pathways in H_2O_2 inhibition of CCh-stimulated Cl^- secretion

Previous studies from our group have shown that CCh-stimulated MAPK activation occurs, at least in part, following activation of the soluble tyrosine kinase, p60Src. Therefore, we next investigated whether Src activation was involved in the inhibitory effect of H_2O_2 on CCh-stimulated Cl^- secretion. Preincubation of T_{84} cells with the Src inhibitor, PP2 (20 μM), significantly reduced the inhibitory effect of H_2O_2 thus indicating at least a partial role for Src activation in H_2O_2-induced inhibition of Ca^{2+}-dependent Cl^- secretion (Fig. 3A; $P<0.05$; $n = 5$). Interestingly, H_2O_2 caused a rapid and sustained increase in Src phosphorylation at position Y416, as determined by Western blot analysis (Fig. 3B; $P<0.05$; $n = 6$). Another soluble tyrosine kinase involved in the negative regulation of Cl^- secretion is the calcium-dependent kinase, Pyk-2. Pyk-2 and Src activation can increase each other's phosphorylation status (30, 46, 47). Consequently, we investigated whether H_2O_2 also increased Pyk-2 activation, as measured by increased phosphorylation of Pyk-2 at the Y881 residue. H_2O_2 induced sustained Pyk-2 phosphorylation in a manner similar to Src activation, albeit with slightly delayed kinetics (Fig. 3C; $P<0.001$; $n = 4$).

H_2O_2 phosphorylates EGFR but does not recruit EGFR to mediate inhibition of Cl^- secretion

As H_2O_2 inhibits CCh-stimulated Cl^- secretion *via* an ERK-dependent pathway and because the EGFR is an upstream regulator of this kinase, we initially investigated whether H_2O_2 could activate EGFR. Bilateral H_2O_2 treatment increased EGFR tyrosine phosphorylation in T_{84} cell monolayers in both a concentration-(Fig. 4A; $P<0.05$–$P<0.001$ *vs.* control; $n = 6$) and a time-dependent (Fig. 4B; $P<0.05$ – $P<0.01$ *vs.* control; $n = 6$) manner. We next investigated the mechanisms by which H_2O_2 stimulated EGFR phosphorylation. Activation of EGFR by H_2O_2 (500 μM) was reduced by pretreatment of cells with either the EGFR kinase inhibitor, tyrphostin AG1478 (1 μM; Fig. 4C; $P<0.01$; $n = 6$), or a neutralizing anti-EGFR antibody (5 μg/ml, $P<0.001$) to block the EGFR ligand-binding domain. These data suggest that H_2O_2 phosphorylates the EGFR *via* the kinase activity of the EGFR itself and through the possible release and binding of an EGFR ligand. Since H_2O_2 inhibition of CCh-stimulated Cl^- secretion is ERK and p38 dependent, we next investigated whether EGFR activation was required for stimulation of these downstream kinases. Preincubation with either tyrphostin AG1478 or a neutralizing antibody against the EGFR-ligand binding domain failed to significantly block activation of ERK or p38 by H_2O_2 (Fig. 4D, E). These data indicate that H_2O_2-induced activation of ERK and p38 occurs independently of EGFR activation. When we investigated whether EGFR activation was involved in the inhibitory effect of H_2O_2 on CCh-stimulated Cl^- secretion, preincubation with tyrphostin AG1478 had no effect on H_2O_2-induced inhibition of CCh-stimulated Cl^- secretion by H_2O_2 (Fig. 4F). These data indicate that EGFR activation is likely not involved in H_2O_2-induced inhibition of Ca^{2+}-dependent Cl^- secretion.

Role of cytosolic calcium ($[Ca^{2+}]_{cyt}$) in signaling events mediated by H_2O_2

An elevation in $[Ca^{2+}]_{cyt}$ levels is one of the major second messengers involved in the prosecretory actions of stimuli such as CCh and other GqPCR agonists. However, $[Ca^{2+}]_{cyt}$

is also involved in the recruitment of antisecretory signaling pathways, including ERK and p38 (27, 41). H_2O_2 has been shown to cause an increase in $[Ca^{2+}]_{cyt}$ levels in some cell systems. In addition, we have shown that H_2O_2 increases activation of the Ca^{2+}-dependent kinase, Pyk-2, which translates elevations in $[Ca^{2+}]_{cyt}$ to a tyrosine kinase-dependent signal. Consequently, we investigated whether H_2O_2 recruitment of signaling pathways involved in the negative regulation of Cl^- secretion required elevations in $[Ca^{2+}]_{cyt}$. In fact, pretreatment of T_{84} monolayers with the $[Ca^{2+}]_{cyt}$ chelator, BAPTA-AM (20 μM), reduced H_2O_2 activation of Src (Fig. 5A; $P<0.05$; $n = 5$) and ERK MAPK (Fig. 5B; $P<0.001$; $n = 4$). In addition, BAPTA-AM also partially reduced p38 activation (Fig. 5C; $P<0.001$; $n = 7$) and blocked Pyk-2 activation (Fig. 5D; $P<0.01$; $n = 5$).

To directly investigate whether H_2O_2 treatment alters $[Ca^{2+}]_{cyt}$ levels, we performed digital calcium imaging by preincubating HT-29.cl19a colonic epithelial cells, grown on coverslips, for 30 min with the Ca^{2+}-dye, Fura-2 (5 μM). HT-29.cl19a cells were used because they gave a robust and stable response to CCh, whereas repeated attempts with T_{84} cells grown on coverslips failed to show a stable response to CCh, possibly because of an inability to access muscarinic receptors that are restricted to the basolateral membrane. In complementary Ussing chamber studies, the I_{sc} response to CCh in HT-29.cl19a cell monolayers pretreated with H_2O_2 (500 μM) was reduced to 39±20% that of the response seen in monolayers treated with CCh alone (4.0±0.5 *vs.* 1.7±1.0 μA/cm^2; $P<0.05$; $n = 3$), a similar level of inhibition as seen in T_{84} cells. HT-29.cl19a cells grown on coverslips were mounted on an imaging stage. H_2O_2 (500 μM) caused a gradual increase in $[Ca^{2+}]_{cyt}$ levels, which reached a plateau (Fig. 6A, B; $P<0.001$; $n = 51$). Since CCh stimulation of ion transport is Ca^{2+}dependent, we then investigated whether H_2O_2 inhibited the ability of CCh to evoke a Ca^{2+} response. Cells grown on coverslips, preloaded with Fura-2, were incubated with H_2O_2 or HBSS for 30 min prior to treatment with CCh. The $[Ca^{2+}]_{cyt}$ response to CCh (Fig. 6C) was partially reduced by H_2O_2 pretreatment (Fig. 6D; $P<0.001$; $n = 51$), but CCh still induced a robust calcium signal, as the level of inhibition by H_2O_2 was only 18±6% (Fig. 6E, $P<0.001$; $n=51$). These data suggest that H_2O_2 likely does not deplete intracellular Ca^{2+} stores sufficiently to block CCh-stimulated increases in $[Ca^{2+}]_{cyt}$ levels that are adequate to drive a chloride secretory response.

Recruitment of multiple regulatory signaling pathways by H_2O_2

The recruitment of signaling molecules involved in the negative regulation of Ca^{2+}-dependent Cl^- secretion also involves stimulus-selective recruitment of specific signaling pathways. One example of this signaling divergence is the recruitment of phosphoinositide 3-kinase (PI3-K) signaling following activation of the EGFR by native ligand, but a lack of PI3-K recruitment following CCh-stimulated EGFR transactivation (48, 49). When we investigated whether PI3-K activation plays a role in mediating the inhibitory effects of H_2O_2 on CCh-stimulated Cl^- secretion, preincubation with the PI3-K inhibitor, wortmannin (50 nM), significantly reduced the inhibitory effect of H_2O_2, thus indicating a prominent role for PI3-K activation in the inhibitory effect of H_2O_2 on Ca^{2+}-dependent Cl^- secretion (Fig. 7A; $P<0.01$; $n = 4$). These data were supported by studies using an alternative PI3-K inhibitor, LY294002 (20 μM). Pre-incubation of T_{84} cells with LY294002 significantly reduced the inhibitory effect of H_2O_2 on CCh-stimulated Cl^- secretion (Fig. 7B; $P<0.05$; $n =$

5). H_2O_2 treatment also activated PI3-K signaling, as measured by increased phosphorylation of the downstream signaling target, Akt1 (Thr 308). This effect was shown to occur, at least in part, in a Ca^{2+}-dependent manner as pretreatment with BAPTA significantly reduced Akt1 phosphorylation (Fig. 7C; $P<0.05$; $n = 4$). However, H_2O_2-stimulated Akt1 activation occurred independently of EGFR kinase activity as the EGFR inhibitor, tyrphostin AG1478, did not significantly inhibit Akt1 activation [7±2arbitrary units in untreated; 20±3 in H_2O_2 treated ($P<0.01$ *vs.* untreated); 9±3 in AG1478 treated; 15±2 in AG1478+H_2O_2 treated cells ($P<0.01$ *vs.* untreated); $n = 5$].

Because both PI3-K and p38 appeared to play prominent roles in mediating the inhibitory effect of H_2O_2 on CCh-stimulated Cl^- secretion, we next investigated whether PI3-K and p38 activation were components of one, or separate, signaling pathways. T_{84} cells were pretreated with either the PI3-K inhibitor, wortmannin, or the p38 inhibitor, SB203580, for 30 min prior to treatment with H_2O_2 for 5 min, a time point where significant phosphorylation of both p38 (*cf.* Fig. 2E) and Akt1 (*cf.* Fig. 7C) had been observed. Wortmannin pretreatment exerted no inhibitory effect on H_2O_2-induced p38 phosphorylation (Fig. 8B; $n = 4$) but did inhibit phosphorylation of the PI3-K downstream target, Akt1, while SB203580 significantly reduced phosphorylation of Akt1 (Fig. 7D; $P<0.01$; $n = 5$). These data suggest that p38 activation in response to H_2O_2 treatment lies upstream of PI3-K.

We next investigated whether H_2O_2-induced ERK activation occurred in sequence or in parallel with the p38-PI3-K activation pathway. Preincubation with the MEK inhibitor, PD98059 (50 μM), significantly blocked H_2O_2-induced ERK phosphorylation (Fig. 8A; $P<0.001$; $n = 3$). However, PD98059 had no significant effect on H_2O_2-induced p38 (Fig. 8B; $n = 4$) or Akt1 phosphorylation (Fig. 8C; $n = 5$). These data suggest that H_2O_2-induced ERK activation does not lie upstream of p38 or PI3-K. Furthermore, the PI3-K inhibitor, wortmannin, which blocked Akt1 phosphorylation (Fig. 8C; $P<0.05$; $n = 5$), had no effect on ERK phosphorylation in response to H_2O_2 (Fig. 8A). This suggests that PI3-K signaling does not influence ERK activation. In addition, wortmannin had no effect on p38 phosphorylation (Fig. 8B), thus supporting our earlier findings that PI3-K lies downstream of p38 (*cf.* Fig. 7D). Collectively, these data demonstrate that H_2O_2 activates two separate signaling pathways that contribute to negative regulation of Ca^{2+}-dependent ion transport responses.

Identity of ion transport proteins targeted by H_2O_2

We next set out to identify specific ion transport proteins that are involved in the inhibitory effect of H_2O_2. The secretory response to CCh is dependent on the activity of a number of ion transport proteins. A basolateral K^+ efflux is essential to maintain the electrochemical gradient required to drive active Cl^- secretion by CCh (50, 51). We therefore investigated whether CCh-stimulated opening of basolateral K^+ channels is affected by H_2O_2 pretreatment. T_{84} monolayers were preloaded with $^{86}Rb^+$, a surrogate for K^+, prior to incubation with H_2O_2 (500 μM) or Ringer's solution for 30 min. Cells were then treated with CCh (100 μM), and $^{86}Rb^+$ efflux was determined at 2-min time intervals. H_2O_2 pretreatment significantly reduced CCh-stimulated 86Rb^+ efflux, by 31 7% (Fig. 9A; $P<0.05$; $n = 4$). Treatment of control monolayers with H_2O_2 alone had no effect on basal

$^{86}Rb^+$ efflux (Fig. 9A). These data imply that H_2O_2 reduces CCh-stimulated opening of basolateral K^+ channels.

Basolateral entry of Cl^- and K^+ into colonic epithelial cells is mediated by the Na^+-K^+-$2Cl^-$ cotransporter, NKCC1, while 3 K^+ ions also enter the cell *via* the energy-consuming Na^+-K^+-ATPase pump in exchange for 2 Na^+ ions (52). The coordinated activation of both of these transporters is required to create the concentration gradient necessary for electrogenic Cl^- secretion to occur. Therefore, we investigated whether H_2O_2 attenuated the secretory response to CCh by inhibiting the influx of K^+ ions. H_2O_2 pretreatment (500 μM; 30 min) had no effect on baseline K^+ influx, as measured by influx of the K^+ surrogate, $86Rb^+$, while acute treatment with H_2O_2 for 1 min also had no effect on K^+ influx (data not shown). However, H_2O_2 did significantly reduce CCh-stimulated K^+ influx by 51±14% (Fig. 9B; $P<0.05$; $n=4$). To investigate the role of NKCC1 in CCh-stimulated K^+ influx, we used the NKCC1 inhibitor, bumetanide (10 μM) to determine the ability of H_2O_2 to inhibit the bumetanide-sensitive component of CCh-stimulated K^+ influx. In the presence of bumetanide, residual uptake of K^+ (bumetanide-insensitive uptake) in CCh-treated tissues was identical in the presence or absence of H_2O_2. When the bumetanide-insensitive component was subtracted from the total K^+ uptake to yield the bumetanide-sensitive K^+ uptake, CCh-stimulated uptake was completely blocked in H_2O_2 pretreated cells. These data indicate that H_2O_2 strongly inhibits CCh-stimulated NKCC1 activity. During the transition to the secreting state, activation of NKCC1 *via* phosphorylation depends critically on the decrease in intracellular Cl^- concentration that accompanies regulated apical Cl^- exit (53). To determine whether the inhibitory effect of H_2O_2 on NKCC1 activity occurred secondary to inhibition of apical Cl^- channels, we measured K^+ influx in Cl^--depleted T_{84} cells. This was accomplished by preincubating T_{84} cells in a Cl^--free isethionate medium prior to treatment with H_2O_2. In unstimulated Cl^--depleted cells, K^+ influx was 2.8-fold higher than in control cells containing normal Cl^- (*cf.* Fig. 9B), and CCh did not induce a further increase in K^+ uptake. The elevated basal K^+ influx presumably reflected a stimulation of NKCC1 in response to Cl^- depletion alone (Fig. 9C). The elevated uptake of K^+ was inhibited by H_2O_2 pretreatment ($P<0.05$; $n=9$). In the presence of bumetanide, the bumetanide-insensitive uptake was equivalent under all four treatment conditions. The bumetanide-sensitive uptake of K^+ in control and CCh-treated cells was dramatically inhibited by H_2O_2 pretreatment ($P<0.05$; $n=9$). This demonstrates that when the contribution of apical Cl^- efflux to NKCC1 activation is removed, H_2O_2 still inhibits NKCC1 activity. Therefore, these data strongly suggest that H_2O_2 inhibits NKCC1 independently of possible alterations in intracellular Cl^- concentration.

DISCUSSION

In the present study, we have demonstrated that H_2O_2 inhibits Ca^{2+}-dependent epithelial Cl^- secretion by activating specific signaling pathways that inhibit membrane ion transport proteins. This inhibitory effect supports previous findings of H_2O_2 inhibition of cAMP-dependent Cl^- secretion (25). Moreover, in agreement with these studies, H_2O_2 (500 μM) had no effect on T_{84} transepithelial resistance, in contrast to the effects of incubation for longer durations or with higher concentrations of H_2O_2 (15, 24). This indicates that our observed effects of H_2O_2 on ion transport regulation are not due to nonspecific damage to

the epithelial monolayer. Other groups have observed stimulatory effects of H_2O_2 on epithelial I_{sc}. We did not detect a significant stimulatory effect of H_2O_2 on epithelial ion transport (not shown). Our findings and those of other groups suggest that at lower experimental concentrations (*i.e.*, 500 μM), H_2O_2 exerts an inhibitory effect on I_{sc}, whereas at higher concentrations (*i.e.*, 2.2–5.5 mM), a small stimulatory response can occur (24).

H_2O_2 has emerged as an important transducer of cellular signals, including mediating responses to growth factors such as EGF (54), as well as participating in the activation of MAPK and NF-κB signaling pathways (55, 56). In addition, we have previously established the involvement of EGFR and MAPK pathways in the regulation of Ca^{2+}-dependent Cl^- secretion in intestinal epithelial cells (31, 43, 46, 48, 57). Here, we observed that H_2O_2 activated a number of discreet signaling pathways that occurred, at least in part, downstream of elevations in cytosolic Ca^{2+}levels. H_2O_2 has been shown in a number of systems to modify $[Ca^{2+}]_{cyt}$ concentrations (58, 59). Indeed, the pattern of a slow and sustained elevation in $[Ca^{2+}]_{cyt}$, similar to that seen in Fig. 6A, has been described in H_2O_2-treated pancreatic acinar cells (60). At this stage, we have not identified the H_2O_2-responsive Ca^{2+} pool that was activated in these studies, or whether H_2O_2 increases the influx of extracellular Ca^{2+}.

The elevation in $[Ca^{2+}]_{cyt}$ was not sufficient to prevent CCh from mounting a robust Ca^{2+} response. This fact is important from the perspective of continued Ca^{2+}-dependent processes in the face of exposure to an inflammatory mediator. Moreover, H_2O_2-induced elevations in $[Ca^{2+}]_{cyt}$ were able to activate two separate signaling pathways. We have previously established a role for the Ca^{2+}-responsive soluble kinases, Pyk-2, and Src in the regulation of CCh-stimulated Cl^- secretion (30, 43). In this current study, we similarly observed a role for Ca^{2+} in the activation of ERK MAPK, downstream of Src and Pyk-2, and a separate pathway involving p38 MAPK activation and downstream activation of PI3-K signaling. The kinetics of activation of these signaling kinases correlates with their upstream role in mediating H_2O_2 inhibition of CCh-stimulated I_{sc}, which was highly significant after 15 min pretreatment (*cf.* Fig. 1B). The transient nature of the activation of certain kinases, *i.e.*, ERK, suggests a discrete level of control is in operation to prevent consequences arising from sustained activation of these mediators. We have previously reported the potentiating effect of inhibitors of ERK, p38, PI3-K, and Src, on CCh-stimulated Cl^- secretion. However, in order to clearly demonstrate the role of Src and PI3-K in H_2O_2-mediated inhibition of CCh-stimulated I_{sc}, these data were presented as the % inhibition of CCh-stimulated I_{sc}, consequently masking the definite potentiating effect of PP2 and LY294002 on the CCh response. Although the ERK and p38 inhibitors did not show a clear potentiating effect on CCh-stimulated I_{sc} (in monolayers not treated with H_2O_2), this may have been due to the lower experimental number than used in our previous studies to specifically demonstrate a potentiating effect of ERK and p38 inhibition (31, 46). Interestingly, EGFR, which lies upstream of MAPK signaling in response to a number of stimuli, was not involved in the inhibitory effect of H_2O_2 on CCh-stimulated Cl^- secretion, even though H_2O_2 did increase EGFR phosphorylation. Furthermore, EGFR activation appears to occur *via* the release of an EGFR ligand, as H_2O_2-induced EGFR phosphorylation was dramatically inhibited by a neutralizing antibody against the ligand-binding domain of the EGFR. On the basis of our previous studies of EGFR transactivation in these cells in response to a Ca^{2+}-generating

agonist (CCh), the ligand responsible for H_2O_2-induced EGFR transactivation is likely transforming growth factor-α (TGF-α), although this remains to be confirmed (38). The significance of H_2O_2-induced EGFR activation in these experiments is unclear, although there is conflicting evidence for a protective role of EGFR activation against H_2O_2-induced increases in the permeability of Caco-2 intestinal epithelial monolayers (61, 62). Moreover, the reason why H_2O_2-induced EGFR phosphorylation becomes uncoupled from downstream signaling pathways is unknown but is worthy of additional study.

Two key events involved in the Cl^- secretory response to CCh are the efflux of K^+ ions through basolateral K^+ channels and the NKCC1-mediated ba-solateral uptake of Cl^- ions (in conjunction with Na^+ and K^+) that replenishes intracellular Cl^- lost through apical Cl^- channels. Our data indicate that H_2O_2 inhibits both of these processes. Although DuVall *et al.* (25) demonstrated that acute treatment with H_2O_2 could increase apical to basolateral K^+ transport, we did not observe an increase in basolateral $^{86}Rb^+$ efflux in response to H_2O_2. However, our studies were not conducted in the presence of the Na^+-K^+-ATPase inhibitor, ouabain, which potentiates the basolateral K^+ conductance response by inhibiting reuptake of $^{86}Rb^+$ through the Na^+ pump. Previous studies have demonstrated that H_2O_2 can inhibit cAMP-stimulated apical Cl^- efflux (25, 26). Nevertheless, by depleting T_{84} monolayers of Cl^-, we were able to demonstrate that H_2O_2 inhibits NKCC1 activity independent of effects on apical Cl^- conductance. NKCC1 regulation is mediated in part by phosphorylation of threonine residues on the N terminus of NKCC1 (63–66). Furthermore, internalization of NKCC1 plays an important role in terminating the involvement of NKCC1 in CCh-stimulated ion transport in both cultured colonic epithelial cells and isolated human colonic crypts (67, 68). Interestingly, in Calu-3 airway cells, basolateral application of H_2O_2 potentiated forskolin-stimulated I_{sc} responses by increasing NKCC1 activity, while apical application of H_2O_2 inhibited I_{sc} responses (69). In addition to differences between cAMP- and Ca^{2+}-dependent ion transport, this observation likely reflects inherent differences between airway and intestinal epithelial ion transport processes, as we observed identical levels of inhibition of CCh-stimulated I_{sc} in T_{84} cells exposed solely on the apical or basolateral surface to H_2O_2 (data not shown). The exact nature of NKCC1 regulation by H_2O_2, and the signaling events involved, are the focus of our current studies.

In conclusion, we have demonstrated that pathophysiologically relevant concentrations of H_2O_2 can inhibit Ca^{2+}-dependent Cl^- secretion by activating kinase signaling pathways that negatively regulate ion transport. In addition, H_2O_2 inhibits basolateral K^+ efflux and the uptake of K^+ and Cl^- *via* NKCC1 (Fig. 10). *In vivo*, Ca^{2+}-dependent Cl^- secretion is a critical response to neuronal reflexes activated by changes in luminal contents, distension, and physical contact between the epithelium and luminal contents (70). Reduced Cl^- secretion leads to reduced flushing of the crypt to remove noxious substances and pathogenic bacteria. Therefore, fluid secretion is an important component of the epithelial barrier and host protection, and when secretion is compromised, this likely contributes to a decrease in overall barrier effectiveness. Indeed, the importance of Cl^- secretion was emphasized in a recent study demonstrating that inhibition of the CFTR Cl^- channel in isolated airway epithelial cells induces an inflammatory profile similar to that observed in cystic fibrosis (71). Therefore, dysregulation of ion transport can strongly influence the inflammatory status of the mucosa. The diarrhea associated with IBD is believed to be due

primarily to defective solute and fluid absorption, thus leading to retention of fluid in the lumen, rather than an excess of active secretion (19, 72, 73). Although most studies on ion transport defects in human and murine colitis have focused on altered expression of ion transport proteins as the primary cause of defective transport, we, and others have previously demonstrated that the ion-transporting properties of isolated tissues from mouse models of colitis can be restored, at least in part, by acute modification of regulatory signaling pathways, including those investigated in this study (26, 74). Therefore, in addition to defects in the structural integrity of the epithelial barrier itself (28, 75), inhibition of fluid secretion, through altered expression and/or regulation of ion transport proteins, might play an important role in facilitating bacterial colonization of the intestinal crypt and the consequent excessive inflammatory response associated with IBD.

Acknowledgments

We gratefully acknowledge the technical assistance of Linh Pham, Anahita Dashtei, and Sameer Gupta (University of California, San Diego). This research was funded by a Crohn's and Colitis Career Development Award (to D.F.M.) and U.S. National Institutes of Health grant DK-28305 (to K.E.B.).

References

1. Grisham MB, Yamada T. Neutrophils, nitrogen oxides, and inflammatory bowel disease. Ann N Y Acad Sci. 1992; 664:103–115. [PubMed: 1456643]
2. Pavlick KP, Laroux FS, Fuseler J, Wolf RE, Gray L, Hoffman J, Grisham MB. Role of reactive metabolites of oxygen and nitrogen in inflammatory bowel disease. Free Radic Biol Med. 2002; 33:311–322. [PubMed: 12126753]
3. Conner EM, Grisham MB. Inflammation, free radicals, and antioxidants. Nutrition. 1996; 12:274–277. [PubMed: 8862535]
4. Grisham MB. Oxidants and free radicals in inflammatory bowel disease. Lancet. 1994; 344:859–861. [PubMed: 7916405]
5. Harris ML, Schiller HJ, Reilly PM, Donowitz M, Grisham MB, Bulkley GB. Free radicals and other reactive oxygen metabolites in inflammatory bowel disease: cause, consequence or epiphenomenon. Pharmacol Ther. 1992; 53:375–408. [PubMed: 1409852]
6. Lih-Brody L, Powell SR, Collier KP, Reddy GM, Cerchia R, Kahn E, Weissman GS, Katz S, Floyd RA, McKinley MJ, Fisher SE, Mullin GE. Increased oxidative stress and decreased antioxidant defenses in mucosa of inflammatory bowel disease. Dig Dis Sci. 1996; 41:2078–2086. [PubMed: 8888724]
7. Kruidenier L, Kuiper I, Van Duijn W, Mieremet-Ooms MA, van Hogezand RA, Lamers CB, Verspaget HW. Imbalanced secondary mucosal antioxidant response in inflammatory bowel disease. J Pathol. 2003; 201:17–27. [PubMed: 12950013]
8. Holmes EW, Yong SL, Eiznhamer D, Keshavarzian A. Glutathione content of colonic mucosa: evidence for oxidative damage in active ulcerative colitis. Dig Dis Sci. 1998; 43:1088–1095. [PubMed: 9590426]
9. Keshavarzian A, Haydek J, Zabihi R, Doria M, D'Astice M, Sorenson JR. Agents capable of eliminating reactive oxygen species. Catalase, WR-2721, or Cu(II)2(3,5-DIPS)4 decrease experimental colitis. Dig Dis Sci. 1992; 37:1866–1873. [PubMed: 1335406]
10. Choudhary S, Keshavarzian A, Yong S, Wade M, Bocckino S, Day BJ, Banan A. Novel antioxidants zolimid and AEOL11201 ameliorate colitis in rats. Dig Dis Sci. 2001; 46:2222–2230. [PubMed: 11680601]
11. Oz HS, Chen TS, McClain CJ, de Villiers WJ. Antioxidants as novel therapy in a murine model of colitis. J Nutr Biochem. 2005; 16:297–304. [PubMed: 15866230]
12. Test ST, Weiss SJ. Quantitative and temporal characterization of the extracellular H_2O_2 pool generated by human neutrophils. J Biol Chem. 1984; 259:399–405. [PubMed: 6323407]

13. Klebanoff, SJ. Oxygen metabolites from phagocytes. In: Gallin, JI.Goldstein, IM., Snyderman, R., editors. Inflammation: Basic Principles and Clinical Correlates. Raven Press; New York: 1992. p. 541-588.
14. Radi R, Beckman JS, Bush KM, Freeman BA. Peroxynitrite oxidation of sulfhydryls. The cytotoxic potential of superoxide and nitric oxide. J Biol Chem. 1991; 266:4244–4250. [PubMed: 1847917]
15. Watson AJ, Askew JN, Sandle GI. Characterisation of oxidative injury to an intestinal cell line (HT-29) by hydrogen peroxide. Gut. 1994; 35:1575–1581. [PubMed: 7828976]
16. Kachur JF, Won-Kim S, Anglin C, Gaginella TS. Eicosanoids and histamine mediate C5a-induced electrolyte secretion in guinea pig ileal mucosa. Inflammation. 1995; 19:717–725. [PubMed: 8595937]
17. Keely SJ, Stack WA, O'Donoghue DP, Baird AW. Regulation of ion transport by histamine in human colon. Eur J Pharmacol. 1995; 279:203–209. [PubMed: 7556402]
18. McCole DF, Otti B, Newsholme P, Baird AW. Complement activation of electrogenic ion transport in isolated rat colon. Biochem Pharmacol. 1997; 54:1133–1137. [PubMed: 9464456]
19. Sandle GI, Higgs N, Crowe P, Marsh MN, Venkatesan S, Peters TJ. Cellular basis for defective electrolyte transport in inflamed human colon. Gastroenterology. 1990; 99:97–105. [PubMed: 2344946]
20. Kachur JF, Keshavarzian A, Sundaresan R, Doria M, Walsh R, de las Alas MM, Gaginella TS. Colitis reduces short-circuit current response to inflammatory mediators in rat colonic mucosa. Inflammation. 1995; 19:245–259. [PubMed: 7541393]
21. Gaginella TS, Kachur JF, Tamai H, Keshavarzian A. Reactive oxygen and nitrogen metabolites as mediators of secretory diarrhea. Gastroenterology. 1995; 109:2019–2028. [PubMed: 7498670]
22. Karayalcin SS, Sturbaum CW, Wachsman JT, Cha JH, Powell DW. Hydrogen peroxide stimulates rat colonic prostaglandin production and alters electrolyte transport. J Clin Invest. 1990; 86:60–68. [PubMed: 2164049]
23. Tamai H, Kachur JF, Baron DA, Grisham MB, Gaginella TS. Monochloramine, a neutrophil-derived oxidant, stimulates rat colonic secretion. J Pharmacol Exp Ther. 1991; 257:887–894. [PubMed: 2033526]
24. Nguyen TD, Canada AT. Modulation of human colonic T84 cell secretion by hydrogen peroxide. Biochem Pharmacol. 1994; 47:403–410. [PubMed: 8304984]
25. DuVall MD, Guo Y, Matalon S. Hydrogen peroxide inhibits cAMP-induced Cl^- secretion across colonic epithelial cells. Am J Physiol Cell Physiol. 1998; 275:C1313–C1322.
26. Walker J, Jijon HB, Churchill T, Kulka M, Madsen KL. Activation of AMP-activated protein kinase reduces cAMP-mediated epithelial chloride secretion. Am J Physiol Gastrointest Liver Physiol. 2003; 285:G850–G860. [PubMed: 12869384]
27. Grisham MB, Gaginella TS, von Ritter C, Tamai H, Be RM, Granger DN. Effects of neutrophil-derived oxidants on intestinal permeability, electrolyte transport, and epithelial cell viability. Inflammation. 1990; 14:531–542. [PubMed: 2174408]
28. Söderholm JD, Olaison G, Peterson KH, Franzén LE, Lindmark T, Wirén M, Tagesson C, Sjödahl R. Augmented increase in tight junction permeability by luminal stimuli in the non-inflamed ileum of Crohn's disease. Gut. 2002; 50:307–313. [PubMed: 11839706]
29. Tamai H, Gaginella TS, Kachur JF, Musch MW, Chang EB. Ca-mediated stimulation of Cl secretion by reactive oxygen metabolites in human colonic T84 cells. J Clin Invest. 1992; 89:301–307. [PubMed: 1729277]
30. Keely SJ, Calandrella SO, Barrett KE. Carbachol-stimulated transactivation of epidermal growth factor receptor and mitogen-activated protein kinase in T(84) cells is mediated by intracellular Ca^{2+}, PYK-2, and p60(src). J Biol Chem. 2000; 275:12619–12625. [PubMed: 10777553]
31. Keely SJ, Uribe JM, Barrett KE. Carbachol stimulates transactivation of epidermal growth factor receptor and mitogen-activated protein kinase in T84 cells. Implications for carbachol-stimulated chloride secretion. J Biol Chem. 1998; 273:27111–27117. [PubMed: 9765228]
32. Weymer A, Huott P, Liu W, McRoberts JA, Dharmsathaphorn K. Chloride secretory mechanism induced by prostaglandin E1 in a colonic epithelial cell line. J Clin Invest. 1985; 76:1828–1836. [PubMed: 2997290]

33. Augeron C, Laboisse CL. Emergence of permanently differentiated cell clones in a human colonic cancer cell line in culture after treatment with sodium butyrate. Cancer Res. 1984; 44:3961–3969. [PubMed: 6744312]
34. Cartwright CA, McRoberts JA, Mandel KG, Dharmsathaphorn K. Synergistic action of cyclic adenosine monophosphate- and calcium-mediated chloride secretion in a colonic epithelial cell line. J Clin Invest. 1985; 76:1837–1842. [PubMed: 2997291]
35. Resta-Lenert S, Barrett KE. Enteroinvasive bacteria alter barrier and transport properties of human intestinal epithelium: role of iNOS and COX-2. Gastroenterology. 2002; 122:1070–1087. [PubMed: 11910358]
36. Shiratsuchi H, Basson MD. Activation of p38 MAP-Kalpha by extracellular pressure mediates the stimulation of macrophage phagocytosis by pressure. Am J Physiol Cell Physiol. 2005; 288:C1083–C1093. [PubMed: 15625302]
37. Dong H, Sellers ZM, Smith A, Chow JY, Barrett KE. Na^+/Ca^{2+} exchange regulates Ca^{2+}-dependent duodenal mucosal ion transport and HCO_3^- secretion in mice. Am J Physiol Gastrointest Liver Physiol. 2005; 288:G457–G465. [PubMed: 15499079]
38. Smith AJ, Chappell AE, Buret AG, Barrett KE, Dong H. 5-Hydroxytryptamine contributes significantly to a reflex pathway by which the duodenal mucosa protects itself from gastric acid injury. FASEB J. 2006; 20:2486–2495. [PubMed: 17142798]
39. Venglarik CJ, Bridges RJ, Frizzell RA. A simple assay for agonist-regulated Cl^- and K conductances in salt-secreting epithelial cells. Am J Physiol Cell Physiol. 1990; 259:C358–C364.
40. Matthews JB, Awtrey CS, Madara JL. Microfilament-dependent activation of $Na^+/K^+/2Cl$-cotransport by cAMP in intestinal epithelial monolayers. J Clin Invest. 1992; 90:1608–1613. [PubMed: 1328303]
41. Owen NE, Prastein ML. Na/K/Cl cotransport in cultured human fibroblasts. J Biol Chem. 1985; 260:1445–1451. [PubMed: 2981857]
42. Rao R, Baker RD, Baker SS. Inhibition of oxidant-induced barrier disruption and protein tyrosine phosphorylation in Caco-2 cell monolayers by epidermal growth factor. Biochem Pharmacol. 1999; 57:685–695. [PubMed: 10037455]
43. McCole DF, Keely SJ, Coffey RJ, Barrett KE. Transactivation of the epidermal growth factor receptor in colonic epithelial cells by carbachol requires extracellular release of transforming growth factor-alpha. J Biol Chem. 2002; 277:42603–42612. [PubMed: 12202486]
44. Basuroy S, Seth A, Elias B, Naren AP, Rao R. MAPK interacts with occludin and mediates EGF-induced prevention of tight junction disruption by hydrogen peroxide. Biochem J. 2006; 393:69–77. [PubMed: 16134968]
45. Kim YM, Song EJ, Seo J, Kim HJ, Lee KJ. Proteomic analysis of tyrosine phosphorylations in vascular endothelial growth factor- and reactive oxygen species-mediated signaling pathway. J Proteome Res. 2007; 6:593–601. [PubMed: 17269716]
46. Keely SJ, Barrett KE. p38 mitogen-activated protein kinase inhibits calcium-dependent chloride secretion in T84 colonic epithelial cells. Am J Physiol Cell Physiol. 2003; 284:C339–C348. [PubMed: 12388102]
47. Dikic I, Tokiwa G, Lev S, Courtneidge SA, Schlessinger J. A role for Pyk2 and Src in linking G-protein-coupled receptors with MAP kinase activation. Nature. 1996; 383:547–550. [PubMed: 8849729]
48. McCole DF, Truong A, Bunz M, Barrett KE. Consequences of direct versus indirect activation of epidermal growth factor receptor in intestinal epithelial cells are dictated by protein-tyrosine phosphatase 1B. J Biol Chem. 2007; 282:13303–13315. [PubMed: 17339316]
49. Uribe JM, Keely SJ, Traynor-Kaplan AE, Barrett KE. Phosphatidylinositol 3-kinase mediates the inhibitory effect of epidermal growth factor on calcium-dependent chloride secretion. J Biol Chem. 1996; 271:26588–26595. [PubMed: 8900131]
50. Dharmsathaphorn K, Pandol SJ. Mechanism of chloride secretion induced by carbachol in a colonic epithelial cell line. J Clin Invest. 1986; 77:348–354. [PubMed: 3003156]
51. Hirota CL, McKay DM. Cholinergic regulation of epithelial ion transport in the mammalian intestine. Br J Pharmacol. 2006; 149:463–479. [PubMed: 16981004]

52. Barrett KE, Keely SJ. Chloride secretion by the intestinal epithelium: molecular basis and regulatory aspects. Annu Rev Physiol. 2000; 62:535–572. [PubMed: 10845102]
53. Lytle C, Forbush B. Regulatory phosphorylation of the secretory Na-K-Cl cotransporter: modulation by cytoplasmic Cl. Am J Physiol Cell Physiol. 1996; 270:C437–C448.
54. Bae YS, Kang SW, Seo MS, Baines IC, Tekle E, Chock PB, Rhee SG. Epidermal growth factor (EGF)-induced generation of hydrogen peroxide. Role in EGF receptor-mediated tyrosine phosphorylation. J Biol Chem. 1997; 272:217–221. [PubMed: 8995250]
55. Guyton KZ, Liu Y, Gorospe M, Xu Q, Holbrook NJ. Activation of mitogen-activated protein kinase by H_2O_2. Role in cell survival following oxidant injury. J Biol Chem. 1996; 271:4138–4142. [PubMed: 8626753]
56. Schreck R, Rieber P, Baeuerle PA. Reactive oxygen intermediates as apparently widely used messengers in the activation of the NF-κB transcription factor and HIV-1. EMBO J. 1991; 10:2247–2258. [PubMed: 2065663]
57. Uribe JM, Gelbmann CM, Traynor-Kaplan AE, Barrett KE. Epidermal growth factor inhibits Ca^{2+}-dependent Cl^- transport in T84 human colonic epithelial cells. Am J Physiol Cell Physiol. 1996; 271:C914–C922.
58. Zheng Y, Shen X. H_2O_2 directly activates inositol 1,4,5-trisphosphate receptors in endothelial cells. Redox Rep. 2005; 10:29–36. [PubMed: 15829109]
59. González A, Granados MP, Pariente JA, Salido GM. H_2O_2 mobilizes Ca^{2+} from agonist- and thapsigargin-sensitive and insensitive intracellular stores and stimulates glutamate secretion in rat hippocampal astrocytes. Neurochem Res. 2006; 31:741–750. [PubMed: 16794860]
60. Granados MP, Salido GM, González A, Pariente JA. Dose-dependent effect of hydrogen peroxide on calcium mobilization in mouse pancreatic acinar cells. Biochem Cell Biol. 2006; 84:39–48. [PubMed: 16462888]
61. Banan A, Choudhary S, Zhang Y, Fields JZ, Keshavarzian A. Oxidant-induced intestinal barrier disruption and its prevention by growth factors in a human colonic cell line: role of the microtubule cytoskeleton. Free Radic Biol Med. 2000; 28:727–738. [PubMed: 10754268]
62. Forsyth CB, Banan A, Farhadi A, Fields JZ, Tang Y, Shaikh M, Zhang LJ, Engen PA, Keshavarzian A. Regulation of oxidant-induced intestinal permeability by metalloprotease-dependent epidermal growth factor receptor signaling. J Pharmacol Exp Ther. 2007; 321:84–97. [PubMed: 17220428]
63. Payne JA, Xu JC, Haas M, Lytle CY, Ward D, Forbush B 3rd. Primary structure, functional expression, and chromosomal localization of the bumetanide-sensitive Na-K-Cl cotransporter in human colon. J Biol Chem. 1995; 270:17977–17985. [PubMed: 7629105]
64. Lytle C. Activation of the avian erythrocyte Na-K-Cl cotransport protein by cell shrinkage, cAMP, fluoride, and calyculin-A involves phosphorylation at common sites. J Biol Chem. 1997; 272:15069–15077. [PubMed: 9182525]
65. Darman RB, Forbush B. A regulatory locus of phosphorylation in the N terminus of the Na-K-Cl cotransporter, NKCC1. J Biol Chem. 2002; 277:37542–37550. [PubMed: 12145304]
66. Dowd BF, Forbush B. PASK (prolinealanine-rich STE20-related kinase), a regulatory kinase of the Na-K-Cl cotransporter (NKCC1). J Biol Chem. 2003; 278:27347–27353. [PubMed: 12740379]
67. Del Castillo IC, Fedor-Chaiken M, Song JC, Starlinger V, Yoo J, Matlin KS, Matthews JB. Dynamic regulation of Na^+-K^+-$2Cl^-$ cotransporter surface expression by PKC-å in Cl^-–secretory epithelia. Am J Physiol Cell Physiol. 2005; 289:C1332–C1342. [PubMed: 16000638]
68. Reynolds A, Parris A, Evans LA, Lindqvist S, Sharp P, Lewis M, Tighe R, Williams MR. Dynamic and differential regulation of NKCC1 by calcium and cAMP in the native human colonic epithelium. J Physiol. 582:507–524.
69. Ohashi T, Ito Y, Matsuno T, Sato S, Shimokata K, Kume H. Paradoxical effects of hydrogen peroxide on human airway anion secretion. J Pharmacol Exp Ther. 2006; 318:296–303. [PubMed: 16569755]
70. Cooke HJ. Enteric tears: Chloride secretion and its neural regulation. News Physiol Sci. 1998; 13:269–274. [PubMed: 11390802]
71. Perez A, Issler AC, Cotton CU, Kelley TJ, Verkman AS, Davis PB. CFTR inhibition mimics the cystic fibrosis inflammatory profile. Am J Physiol Lung Cell Mol Physiol. 2007; 292:L383–L395. [PubMed: 16920886]

72. Greig E, Sandle GI. Diarrhea in ulcerative colitis. The role of altered colonic sodium transport. Ann N Y Acad Sci. 2000; 915:327–332. [PubMed: 11193595]

73. Schmitz H, Barmeyer C, Gitter AH, Wullstein F, Bentzel CJ, Fromm M, Riecken EO, Schulzke JD. Epithelial barrier and transport function of the colon in ulcerative colitis. Ann N Y Acad Sci. 2000; 915:312–326. [PubMed: 11193594]

74. McCole DF, Rogler G, Varki N, Barrett KE. Epidermal growth factor partially restores colonic ion transport responses in mouse models of chronic colitis. Gastroenterology. 2005; 129:591–608. [PubMed: 16083715]

75. Gassler N, Rohr C, Schneider A, Kartenbeck J, Bach A, Obermüller N, Otto HF, Autschbach F. Inflammatory bowel disease is associated with changes of enterocytic junctions. Am J Physiol Gastrointest Liver Physiol. 2001; 281:G216–G228. [PubMed: 11408275]

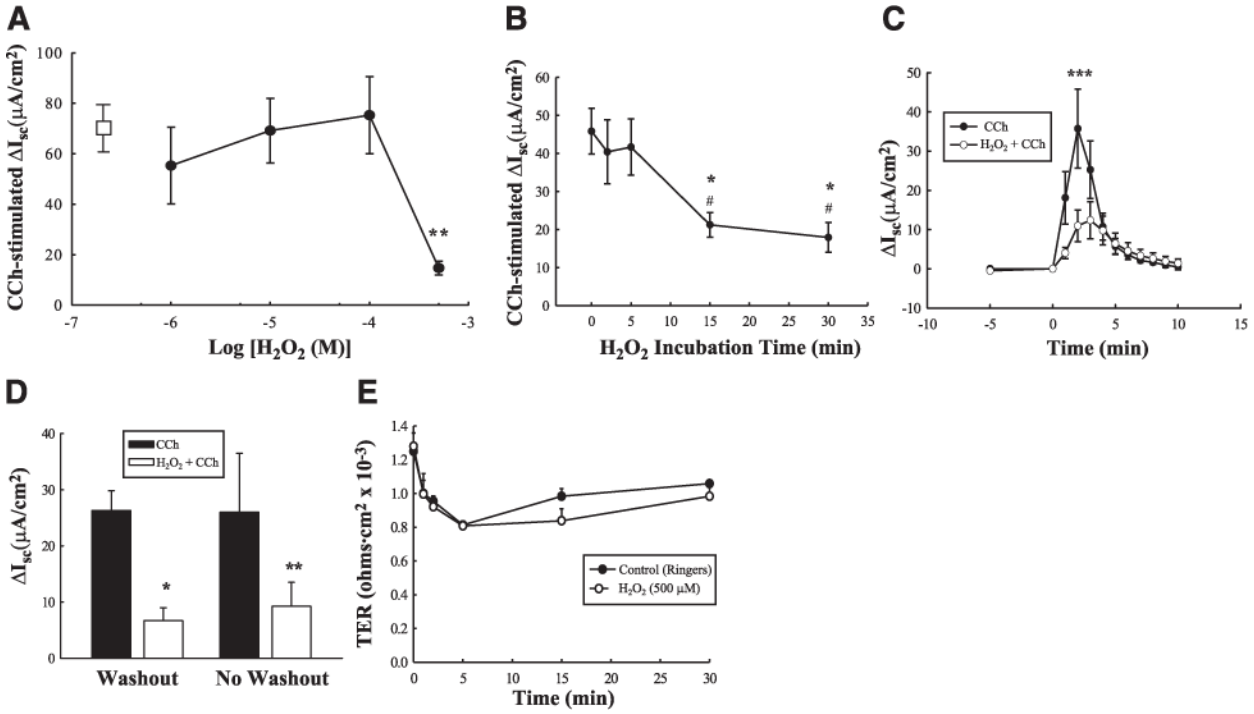

Figure 1.

Hydrogen peroxide (H_2O_2) inhibits carbachol (CCh)-stimulated epithelial I_{sc} without affecting barrier properties. *A*) T_{84} monolayers mounted in Ussing chambers were treated with H_2O_2 (0–500 μM; $n = 6$) for 30 min prior to stimulation of electrogenic Cl^- secretion with CCh. The ΔI_{sc} response to CCh alone is represented by the open rectangle. *B*) Time course of H_2O_2 (500 μM) pretreatment on peak CCh-stimulated I_{sc} (n=4). *C*) Time course of the I_{sc} response to CCh with or without pretreatment for 30 min with H_2O_2 (500 μM; $n = 5$). *D*) Monolayers were pretreated with H_2O_2 (500 μM; 30 min) and treated directly with CCh (no washout), or bathing media were replaced with fresh Ringer's solution, and inserts were then treated with CCh (washout). *E*) Transepithelial resistance across T_{84} monolayers treated with either H_2O_2 (500 μM) for 30 min or Ringer's solution, was measured using a voltohmeter (n=4). Values are presented as means ± SE. * P<0.05; ** P<0.01; *** P<0.001 *vs*. control (CCh alone or untreated cells). $^{\#}P$<0.05 *vs*. 2 min and 5 min H_2O_2 pretreatment on CCh-stimulated I_{sc} (*B*).

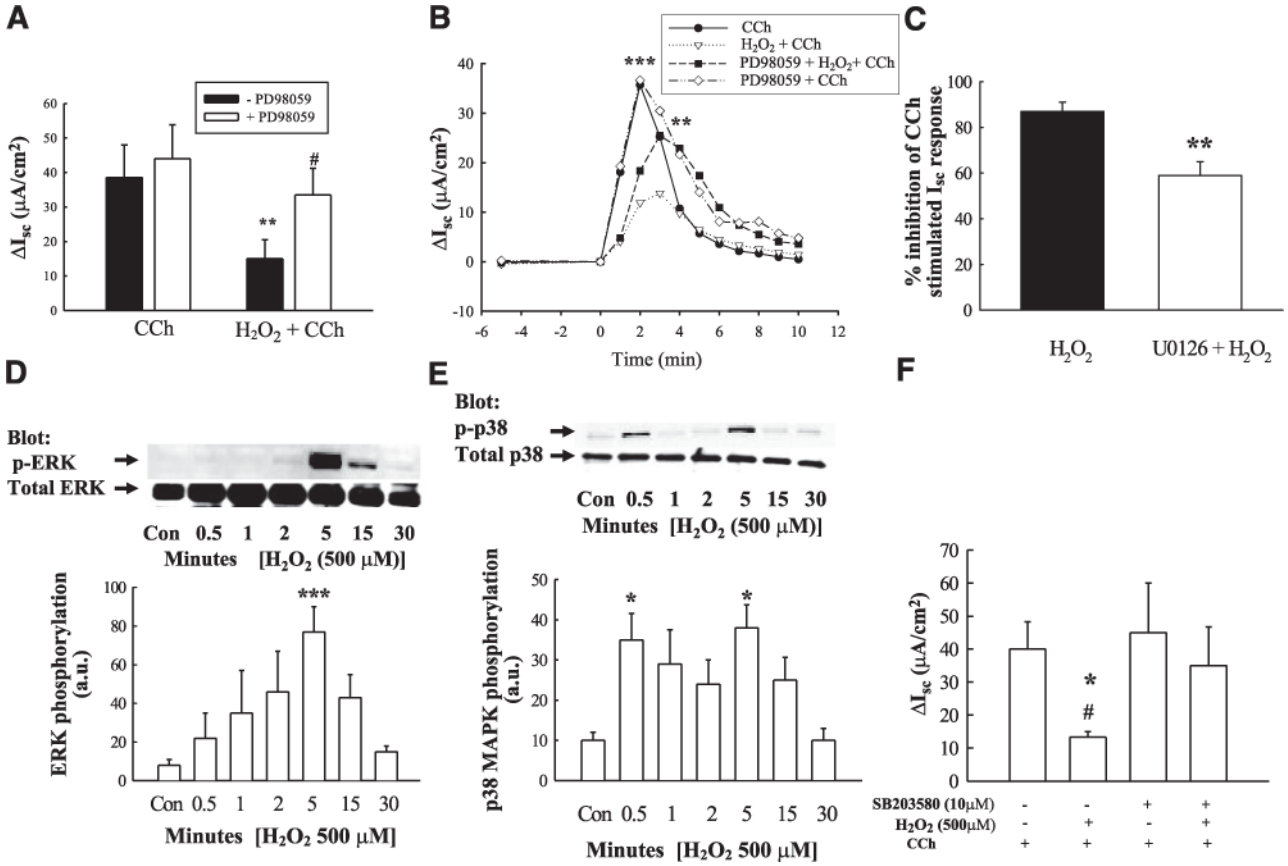

Figure 2.

Inhibition of CCh-stimulated Cl^- secretion involves ERK and p38 MAPK activation. T_{84} monolayers, mounted in Ussing chambers, were preincubated with the MEK inhibitor, PD98059 (*A*, peak ΔI_{sc}; *B*, time course; 50 μM; 30 min; $n = 4$), the MEK inhibitor, U0126 (*C*; 10 μM; 30 min; $n = 6$; data expressed as % inhibition of peak CCh-stimulated I_{sc} response), or the p38 inhibitor, SB203580 (*F*; 10 μM; 30 min; $n = 5$), prior to addition of H_2O_2 (500 μM) or Ringer's solution for 30 min, and subsequent peak I_{sc} responses to CCh (100 μM), and I_{sc} response to CCh over time were measured. Error bars were removed from the time course to aid the clarity of *B*. H_2O_2 induced phosphorylation of ERK (*D*; $n = 5$), and p38 (*E*; $n = 6$) was measured by Western blot and densitometric analyses. Values are presented as means ± SE. $^*P<0.05$; $^{**}P<0.01$; $^{***}P<0.001$ *vs.* control (or H_2O_2 + CCh; *B*, *C*). $^{\#}P<0.05$ *vs.* cells treated with H_2O_2 + CCh (*A*) or H_2O_2 + SB203580 CCh (*F*).

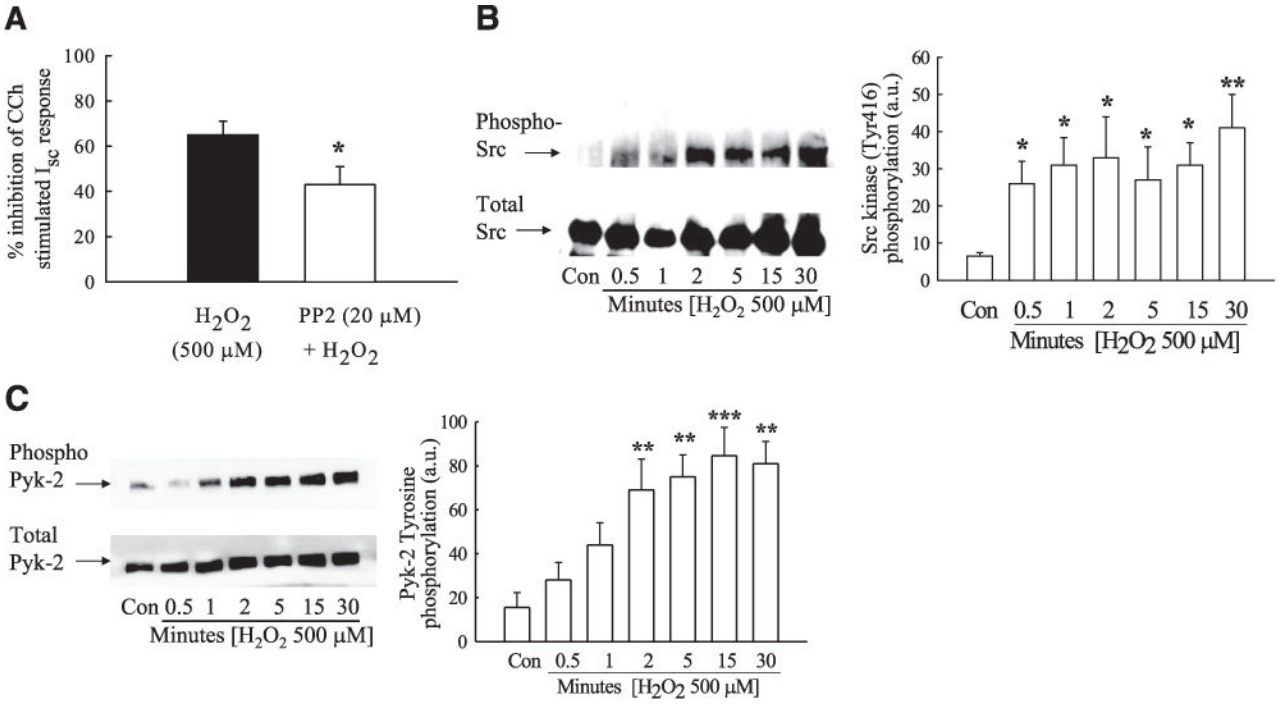

Figure 3.

H_2O_2 induces activation of the Ca^{2+}-responsive kinases, Pyk-2, and Src tyrosine kinase. *A*) T_{84} monolayers were preincubated with the Src kinase inhibitor, PP2 (20 μM; 30 min; $n = 4$) prior to addition of H_2O_2, and subsequent I_{sc} responses to CCh (100 μM) were measured. Data are expressed as percentage inhibition of CCh-stimulated I_{sc} response. *B, C*) H_2O_2 (500 μM)-induced phosphorylation of Src (Y416) (*B*; n=6) and Pyk-2 (Y881) (*C*; n=4), over time (0 –30 min) was determined by Western blot and densitometric analyses. Values are presented as means ± SE. *P<0.05; **P<0.01; ***P<0.001 *vs.* control (H_2O_2 + CCh in *A*; untreated cells in *B, C*).

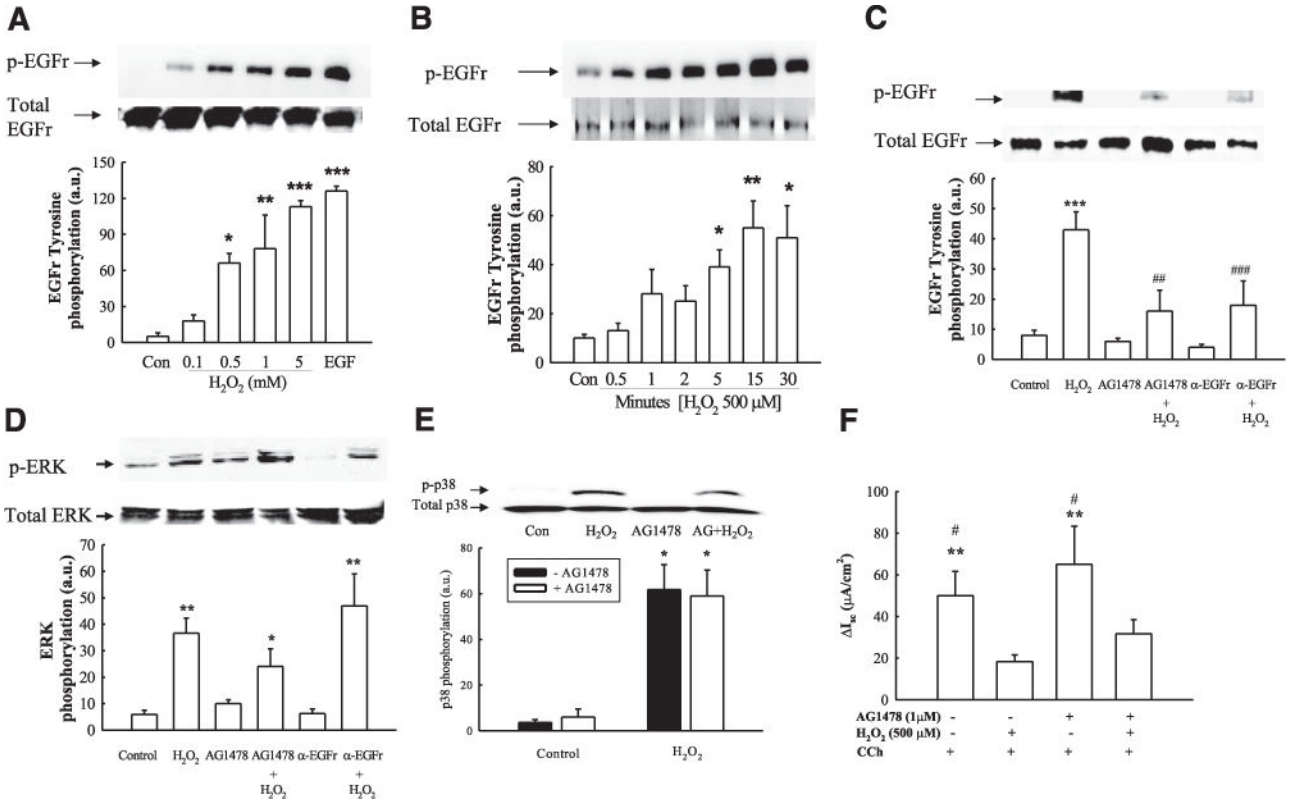

Figure 4.

H_2O_2 stimulates EGFR tyrosine phosphorylation. *A*, *B*) T_{84} monolayers were bilaterally treated with a range of concentrations of H_2O_2 for 5 min (*A*; n=6) or with 500 μM H_2O_2 over different time points (*B*; n=6). EGFR immunoprecipitates were probed for tyrosine phosphorylation levels by Western blot analysis. Bands were quantified by densitometric analysis. *C, D*) Monolayers were preincubated with either the EGFR kinase inhibitor, tyrphostin AG1478 (1 μM), or a neutralizing antibody against the ligand-binding domain of the EGFR (5 μg/ml) to inhibit EGFR activation prior to treatment with H_2O_2. H_2O_2-induced EGFR (*C*; n=6), and ERK phosphorylation (*D*; n=6) was determined by Western blot analysis and densitometry. *E*) T_{84} monolayers were preincubated with tyrphostin AG1478 (1 μM), and H_2O_2-induced p38 phosphorylation was determined by Western blot analysis and densitometry (histogram; n=3). *F*) T_{84} monolayers mounted in Ussing chambers were pretreated with tyrphostin AG1478 (1 μM) prior to addition of H_2O_2, and subsequent I_{sc} responses to CCh (100 μM) were measured (n=6). Results are presented as means ± SE for levels of phosphorylation (a.u., arbitrary units). *P<0.05; **P< 0.01; ***P<0.001 *vs.* control (untreated cells in *A*–*E*; H_2O_2 + CCh in *F*). $^{\#}P$<0.05; $^{\#\#}P$<0.01; $^{\#\#\#}P$<0.001 *vs.* cells treated with H_2O_2 (*C*) or H_2O_2 + AG1478 + CCh (*F*).

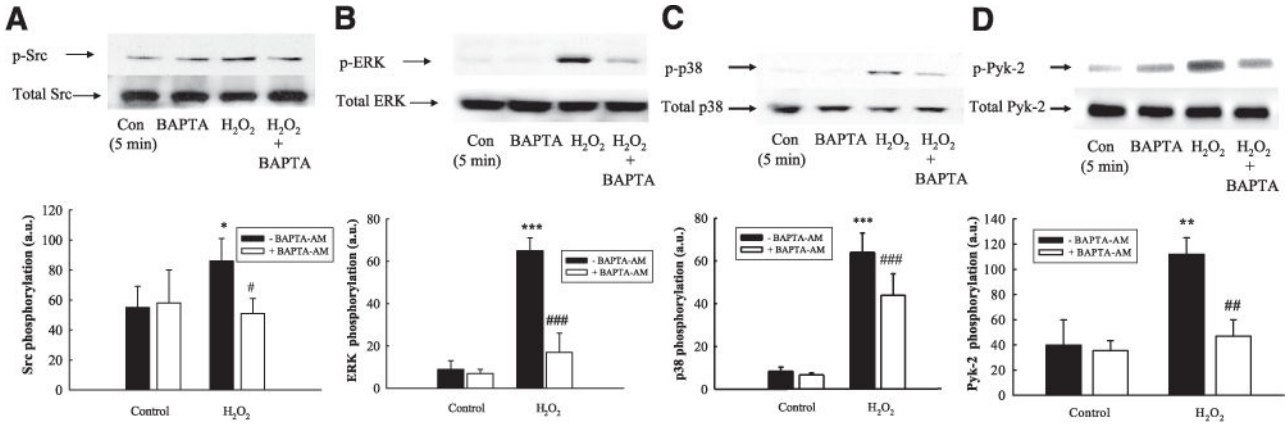

Figure 5.

H_2O_2 increases Src, ERK, and p38 activation in a Ca^{2+}-dependent manner. T_{84} monolayers were preincubated with the Ca^{2+} chelator, BAPTA-AM (20 μM) for 30 min prior to treatment with H_2O_2 (500 μM; 5 min). H_2O_2-induced phosphorylation of Src (Y416) (*A*; n=5), ERK (T202/Y204) (*B*; n=5), p38 (T180/Y182) (*C*; n=7), and Pyk-2 (Y881) (*D*) was assessed by Western blot analysis and subsequent densitometric analysis. Results are presented as means ± SE for levels of phosphorylation (a.u., arbitrary units). **P*<0.05; ***P*<0.01; ****P*<0.001 *vs.* control (untreated cells). $^{\#}P$<0.05; $^{\#\#}P$<0.01; $^{\#\#\#}P$ 0.001 *vs.* cells treated with H_2O_2 alone.

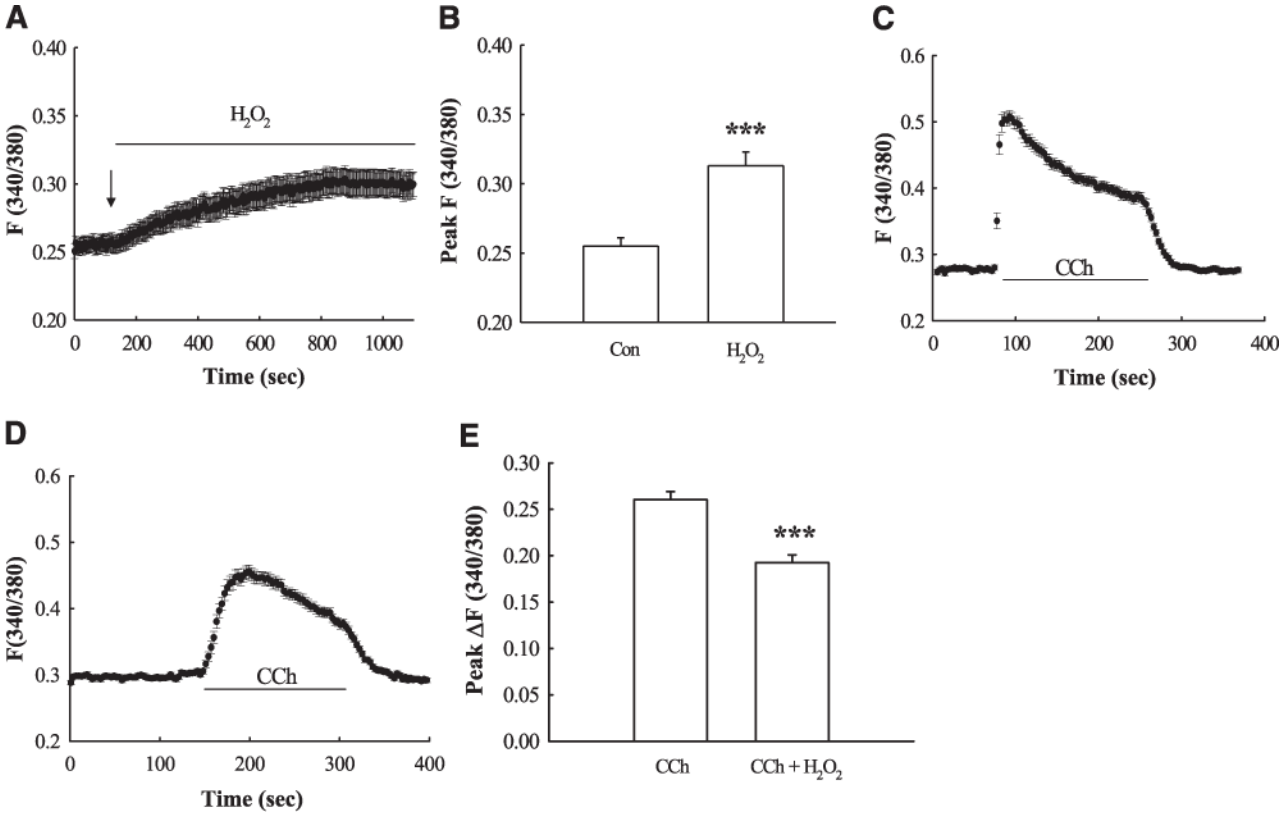

Figure 6.

H_2O_2 increases $[Ca^{2+}]$cyt levels. HT-29.cl19a cells grown on coverslips were preloaded with Fura-2 (5 μM; 30 min) followed by a 60-min wash in HBSS. *A*) Cumulative record of the change in $[Ca^{2+}]$cyt following addition (signified by the arrow) of H_2O_2 (500 μM; n=51). *B*) Peak change in $[Ca^{2+}]$cyt caused by H_2O_2 expressed as the fluorescence ratio, $F_{340/380}$ (n=51). *C*) Cumulative trace of $[Ca^{2+}]$cyt elevation caused by CCh (100 μM; n=51). *D*) Effect of pretreatment of H_2O_2 (30 min) on CCh-stimulated $[Ca^{2+}]$cyt (n=51). *E*) Peak change in CCh-stimulated $[Ca^{2+}]$cyt with or without H_2O_2 pretreatment (n=51). Results are presented as means ± SE. ***P 0.001< *vs.* control or CCh-treated cells.

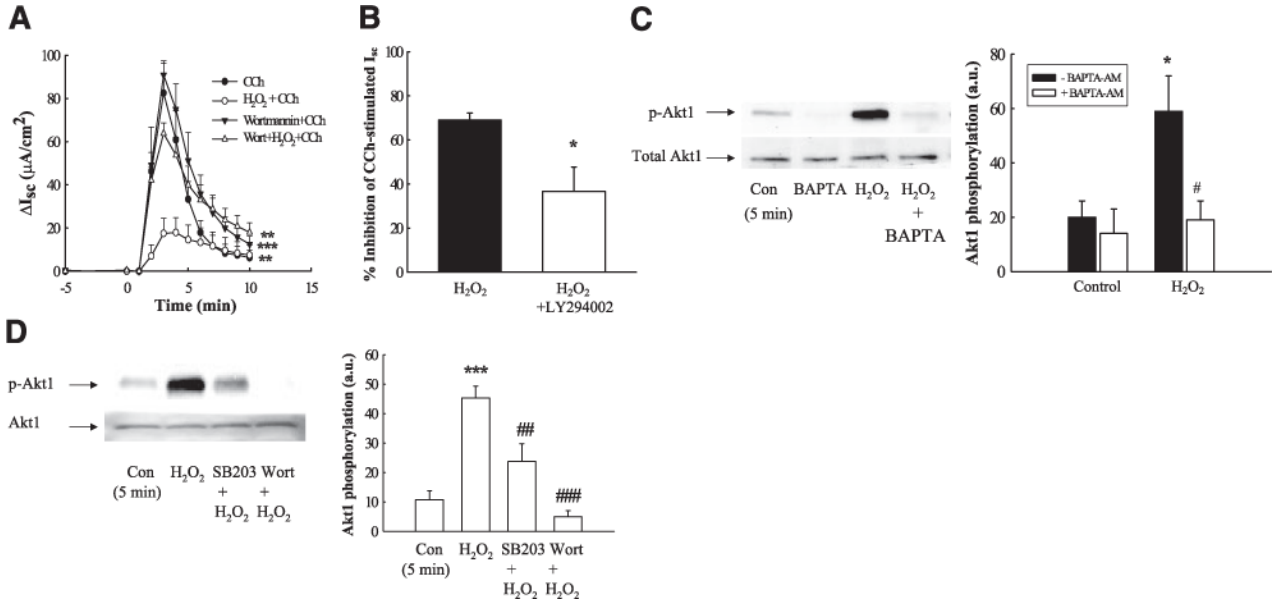

Figure 7.

H_2O_2 inhibition of I_{sc} involves PI3-K activation downstream of p38 activation. *A*) T_{84} monolayers mounted in Ussing chambers were treated with the PI3-K inhibitor, wortmannin (50 nM), for 30 min prior to addition of H_2O_2, and subsequent I_{sc} responses to CCh (100 μM) were measured (n=4). *B*) T_{84} monolayers mounted in Ussing chambers were treated with the PI3-K inhibitor, LY294002 (20 μM), for 30 min prior to addition of H_2O_2, and subsequent I_{sc} responses to CCh (100 μM) were measured (n=4). Data are expressed as percentage inhibition of CCh-stimulated I_{sc} response. *C*) Monolayers were pretreated with BAPTA-AM (20 μM; 30 min) prior to incubation with H_2O_2 (500 μM; 5 min). Lysates were blotted for phosphorylation of the downstream PI3-K target, Akt1 (T308; n=4). *D*) T_{84} monolayers were preincubated for 30 min with the p38 inhibitor, SB203580 (10 μM; n=5), or the PI3-K inhibitor, wortmannin (50 nM; 30 min; n=5), and H_2O_2-stimulated Akt1 phosphorylation was measured. Results are means ± SE for phosphorylation (a.u., arbitrary units). **P*<0.05; ****P*<0.001 *vs.* H_2O_2 + CCh (*A*, *B*) or control (untreated cells; *C, D*). #*P*<0.05; ##*P*<0.01; ###*P*<0.001 *vs.* cells treated with H_2O_2 alone.

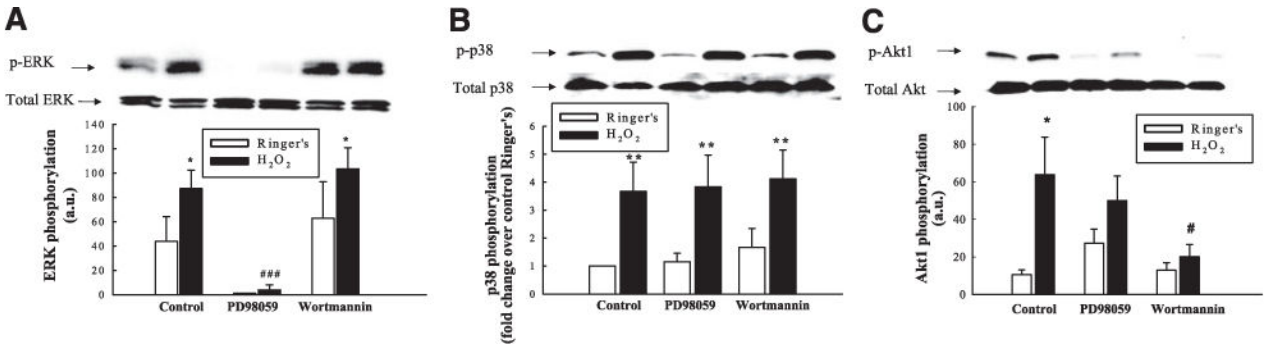

Figure 8.

H_2O_2 activates multiple regulatory signaling pathways. T_{84} monolayers were preincubated with the MEK inhibitor, PD98059 (50 μM), or the PI3-K inhibitor, wortmannin (50 nM), for 30 min prior to treatment with H_2O_2 (500 μM; 5 min). Cell lysates were probed by Western blotting for ERK phosphorylation (*A*; n=3), p38 phosphorylation (*B*; n=4), and Akt1 phosphorylation (*C*; n=5). Results are presented as means ± SE for levels of phosphorylation (a.u., arbitrary units), or fold change over control for p38 phosphorylation (*B*). $^{*}P<0.05$; $^{**}P<0.01$ *vs.* control (untreated cells). $^{\#}P<0.05$; $^{\#\#\#}P<0.001$ *vs.* cells treated with H_2O_2 alone.

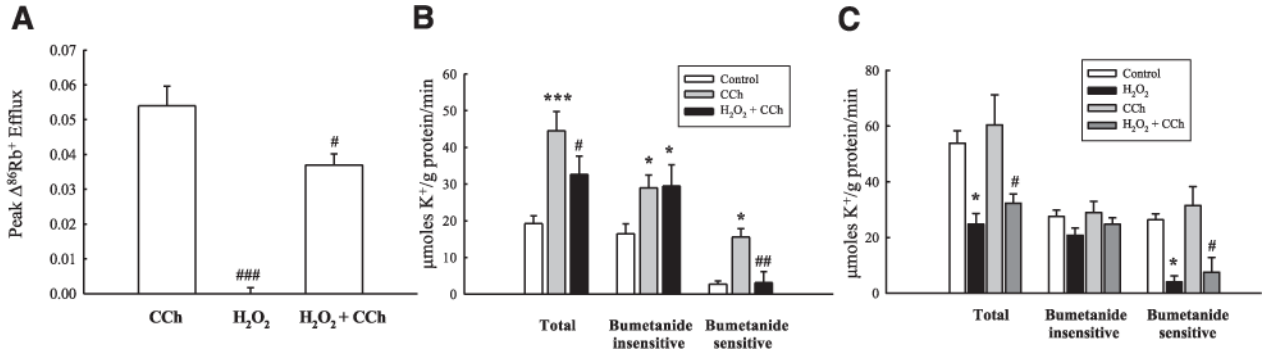

Figure 9.

H_2O_2 inhibits basolateral K^+ efflux and NKCC1 activity. *A*) T_{84} monolayers were preloaded with the K^+ tracer $^{86}Rb^+$ and treated with H_2O_2 (500 µM) bilaterally for 30 min prior to basolateral treatment with CCh. The efflux of $^{86}Rb^+$ into the basolateral bathing solution was measured by scintillation counting. Data were expressed as mean ± SE peak rate of $^{86}Rb^+$ efflux. *B*) T_{84} monolayers were treated with H_2O_2 for 30 min prior to basolateral incubation in CCh for 1 min and transfer to a basolateral $^{86}Rb^+$-containing buffer for 3 min (n=8). The bumetanide insensitive and sensitive components of the response were assessed by incubating inserts in bumetanide (10 µM) concurrently with CCh treatment (n=5). *C*) T_{84} monolayers were depleted of intracellular Cl^- for 60 min prior to treatment as in *B*, but with H_2O_2 and CCh solutions prepared in Cl^--free buffer. Cells were then transferred to basolateral $^{86}Rb^+$ buffer containing Cl^- (n=9). Data are presented as mean ± SE rate of K^+ uptake (µmol K^+/g protein/min). $^*P<0.05$; $^{***}P<0.001$ *vs.* control (untreated cells). $^{\#}P<0.05$; $^{\#\#}P<0.01$; $^{\#\#\#}P<0.001$ *vs.* cells treated with CCh alone.

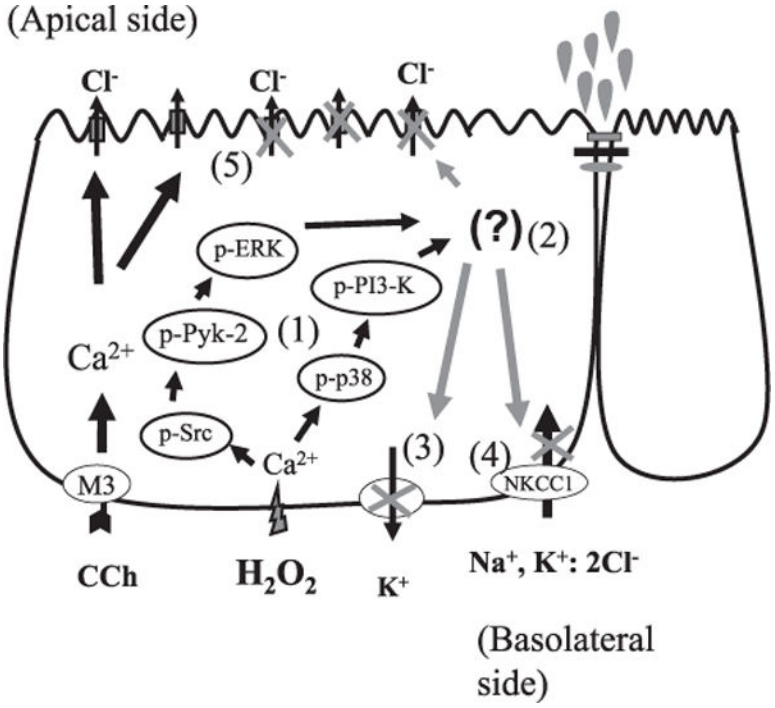

Figure 10.

Integration of H_2O_2-activated regulatory signaling pathways. *1*). H_2O_2 stimulates an increase in cytosolic Ca^{2+} concentration, which triggers two separate kinase pathways that are required for the overall inhibitory effect of H_2O_2 on Ca^{2+}-dependent Cl^- secretion. *2*). Whether these pathways influence different downstream transport processes or converge *via* a downstream signal is unknown. *3*). H_2O_2 also inhibits basolateral Ca^{2+}-responsive K^+ efflux. *4*). H_2O_2 inhibits NKCC1 activity independently of possible effects on apical Cl^- channels. *5*). The inhibition of K^+ efflux and NKCC1 activity likely contributes to the overall inhibitory effect of H_2O_2 on Ca^{2+}-dependent ion transport in colonic epithelial cells.